Molecular Dynamics Studies of the Stability of Water/*n*-Heptane Interfaces with Adsorbed Naphthenic Acids

Zhiying Li, Blair Cranston, Liyan Zhao, and Phillip Choi*

Department of Chemical and Materials Engineering, University of Alberta, Edmonton, Alberta, Canada T6G 2G6

Received: June 7, 2005; In Final Form: August 2, 2005

The mechanism by which naphthenic acids stabilize water/oil interfaces has received extensive attention because of its industrial relevancy. In this work, we employed a molecular dynamics simulation to study its molecular origin. Two models were adopted, wherein naphthenic acid coverage of water/*n*-heptane interfaces, both spherical and flat, was hypothesized, respectively. It was found that the coalescence of two water clusters is entirely attributed to the diffusional motion of the components involved which requires the initial departure of the naphthenic acid molecules from the interface so that a water bridge can form. The naphthenic acids not only act as a steric barrier but also reduce the mobility of the water and *n*-heptane molecules making the formation of the water bridge rather difficult. In fact, our results show that the coalescence of two water clusters fully covered by naphthenic acid molecules is a low-probability event even at evaluated temperatures. In addition, the results from the flat interface models suggest that the emulsion stability is weakly dependent on the molecular weight of the naphthenic acids utilized. Order parameter calculations reveal liquid-crystal-like ordering of naphthenic acids at the water/*n*-heptane interfaces. All these observations are consistent with the corresponding experimental observations. The present work also suggests that the mobility of naphthenic acids is considerably enhanced with more *n*-heptane molecules present outside a water droplet. However, in such a case, coalescence could not occur as the water clusters are far apart from each other.

1. Introduction

This communication is part of a series of molecular dynamics studies of the stability of residual water droplets dispersed in a *n*-heptane continuum phase. The overall objective of the studies is to understand the molecular origin as to why water droplets in certain water-in-oil emulsions encountered in the production and processing of crude oils resist coalescence even at elevated temperatures. In the first communication, we reported that so long as such water clusters are nearby each other, less than 1 nm, local diffusional motions of water molecules would drive them to coalesce in a fraction of a nanosecond at room temperature.[1] The results are somewhat expected as the surface-to-volume ratio of the water clusters used was fairly high. Nevertheless, since the water/oil interfaces of interest usually contain adsorbed surface-active materials and/or fine solids, the previous work, as the first step toward our overall goal, did not provide us with the answer that we are seeking but the experience for modeling such systems.

It has been found that a considerable amount of crude oil produced contains high concentrations of naphthenic acids.[2,3] Since naphthenic acids consist of both hydrophobic and hydrophilic moieties, the materials have been considered as one of the potential candidates, asphaltenes being the other, that could accumulate at the water/oil interface, thereby stabilizing the residual water in crude oils.[4,5] However, if naphthenic acids simply act as a surfactant, it is difficult to explain why such emulsion systems are still fairly stable even at elevated temperatures. Therefore, we decided to apply the molecular dynamics (MD) simulation approach to investigate the molecular origin of the experimental observation. It is hoped that insights obtained from the present molecular modeling study would provide us with some ideas on how to improve the water removal process currently being used.

Stability of model emulsion systems consisting of water, oil, and naphthenic acids/sodium naphthenates has been extensively studied experimentally. In their pioneering work, Friberg et al. proposed that, at high pH values, there exists a lamellar liquid-crystal phase composed of sodium naphthenates at the water/oil interface.[6−10] These authors believe that the observed liquid-crystal phase decreases the mobility of the interface, thereby impeding the occurrence of coalescence. This finding was confirmed by other research groups. In particular, Sjöblom and co-workers studied the effect of pH on the emulsion stability of systems containing naphthenic acids, water, and a *n*-heptane/toluene mixture as the oil phase.[11−17] Their results revealed that emulsion stability increases with increasing pH of the water phase but is weakly dependent on the molecular weight of naphthenic acids. Masliyah et al. also observed the existence of a liquid-crystal-like layer of sodium naphthenates at the interface formed between water and an oil phase composed of a mixture of *n*-heptane and toluene using polarization microscopy,[18−20] and they suggested that there exists a critical concentration of sodium naphthenates in the water phase above which a liquid-crystal-like layer would form. In addition, they constructed phase diagrams of binary solutions consisting of sodium naphthenates and water as well as those of ternary solutions of sodium naphthenates, water, and toluene.

Molecular modeling has been widely used to study emulsion systems with and without surfactants. To the best of our knowledge, most of the studies on systems containing surfactants have focused on flat interfaces rather than on dispersed droplets

* To whom correspondence should be addressed. E-mail: phillip.choi@ualberta.ca. Tel: (780)492-9018. Fax: (780)492-2881.

10.1021/jp053048d CCC: $30.25
Published on Web 10/15/2005

TABLE 1: Equations and Parameters Used in the Modified Drieding 2.21 Force Field

interaction		equation	parameter	
bonded energy (kJ/mol)	bond energy	$E_b = 1/2K_b(R - R_0)^2$	$K_b = 2.93 \times 10^5$ kJ/mol/nm^2 $R_0 = 0.15$ nm	
	angle energy	$E_\theta = 1/2K_\theta(R - R_\theta)^2$	$K_\theta = 418$ kJ/mol/rad^2 $R_\theta = 1.91$ rad	
	torsion energy	$E_\phi = \Sigma_{n=1}^2 1/2K_{\phi,n}[1 \pm \cos(n\phi)]$	$K_\phi = 20.9$ kJ/mol	
	inversion energy	$E_{inv} = K_{inv}(\cos\chi - \cos\chi_0)^2$	$K_{inv} = 20.9$ kJ/mol $\chi_0 = 2.09$ rad	
nonbonded energy (kJ/mol)	coulombic interaction	$E_{coul} = 332.0637q_iq_j/\epsilon r_{ij}erfc(r_{ij}/\beta)$	$\beta = 0.234$ nm $\epsilon = 1$	
	hydrogen bonding	$E_{hb} = \epsilon_0[5(R_0/R)^{12} - 6(R_0/R)^{10}]\cos^4\varphi$	$\epsilon_0 = 16.72$ kJ/mol $R_0 = 0.275$ nm	
	van der Waals energy	$E_{vdw} = \epsilon_0[(\sigma_0/R)^{12} - 2(\sigma_0/R)^6]$	H	$\epsilon_0 = 0.00042$ kJ/mol $\sigma_0 = 0.3195$ nm
			O	$\epsilon_0 = 0.4$ kJ/mol $\sigma_0 = 0.3405$ nm
			C with one implicit H	$\epsilon_0 = 0.6985$ kJ/mol $\sigma_0 = 0.3923$ nm
			C with two implicit H	$\epsilon_0 = 0.6985$ kJ/mol $\sigma_0 = 0.3923$ nm
			C with three implicit H	$\epsilon_0 = 0.6985$ kJ/mol $\sigma_0 = 0.3923$ nm
			off-diagonal interactions	$\epsilon_0 = 1.2607$ kJ/mol $\sigma_0 = 0.4237$ nm

with adsorbed surfactants. For example, Dominguez carried out MD simulations on an ionic/nonionic surfactant mixture adsorbed at the water/carbon tetrachloride interface to study the effect of the surfactant mixture on the interfacial thickness.[21] In fact, studies of this kind usually concentrate on the interfacial thickness, effects of size and molecular structure of the surfactant used on the corresponding interfacial tension, conformation of the surfactant molecules, etc. Urbina-Villalba and co-workers used a Brownian dynamics technique to study the stability of oil-in-water emulsion with the presence of surfactant.[22] However, since not all phases are modeled at the atomistic level in such a technique, it cannot provide a detailed molecular stabilization mechanism. To obtain such information, atomistic Monte Carlo (MC) and MD simulations would probably be the best alternatives even though the present computer resources may limit the size of the system that one can study.

In this work, we employed a molecular dynamics simulation to study the molecular origin of the stabilization mechanism of residue water in oil by naphthenic acids. Two models were adopted in our simulations, wherein naphthenic acid coverage of water/*n*-heptane interfaces, spherical and flat, was hypothesized, respectively. Three issues were addressed: (a) the coalescence mechanism of two nanometer-sized water clusters in *n*-heptane with full coverage of naphthenic acids, (b) the molecular weight dependence of naphthenic acids on the water cluster stability, and (c) the confirmation of the existence of liquid-crystal-like ordering of naphthenic acids at the water/*n*-heptane interface. Moreover, our simulations by using a thick, flat interface with 70 *n*-heptane molecules brought a new light to the role of naphthenic acids in stabilizing the emulsions.

2. Simulation Method and Models

2.1. Force Field. A commercial software package Cerius2, version 4.4, purchased from Accelrys Inc.[23] was used for all MD simulations reported in this communication. Similar to what we used in our previous work,[1] a modified generic force field, Drieding 2.21, developed by Mayo et al.,[24] was used to describe various intra- and intermolecular interactions. The coulombic interactions between the water molecules as well as between the water and naphthenic acid molecules were calculated using the method that an error function was used to achieve a smooth cutoff of the coulombic interaction energy

$$E_{coul} = \frac{332.0637q_iq_j}{\epsilon r_{ij}} erfc\left(\frac{r_{ij}}{\beta}\right) \quad (1)$$

where q_i and q_j are the partial atomic charges in e (1 e = 1.6021 $\times$ 10^{-19} C), which were assigned to every atom by performing the charge equilibration method.[25] The charges for O and H for both the OH groups of the acid and water are in the range of -0.7 to -0.8 and 0.3 to 0.4 e, respectively. The atoms on the hydrophobic tail of the acid molecules were slightly charged, which were also determined by the charge equilibration method. Here, r_{ij} is the distance between atoms i and j in Å, ϵ is the dielectric constant, and a value of 2.34 Å was used for β. The values of the parameters used in the above equation were optimized in order to reproduce the self-diffusion coefficient of water in its pure liquid state. A Lennard-Jones (LJ) 12-10 potential was used to describe the hydrogen bonds formed between water molecules as well as between the water and acid molecules.

For *n*-heptane molecules, a united-atom model was adopted. This means that every CH_3 or CH_2 group was described as one single interaction site. Owing to the nonpolar nature of *n*-heptane, the partial atomic charges were set at zero. Therefore, the van der Waals interaction is the only nonbonded interaction energy to be considered. The van der Waals interaction is expressed as a LJ 12-6 potential. Here, instead of using the default LJ parameters provided by Drieding 2.21, we utilized the parameters developed by Rackaert and Bellemans,[26] which show in our previous work that an accurate heat of vaporization and self-diffusion coefficient of *n*-heptane can be obtained.[1] These LJ parameters along with the default parameters used for the other intramolecular interactions are listed in Table 1. The same set of LJ parameters were used for carbons on the hydrophobic tail of the acids. It should be noted that only hydrogens on the OH groups of the acid molecules were modeled explicitly.

2.2. Molecular Models and Simulation Details. The model construction procedure for our previous study[1] of the coalescence of two nanometer-sized water clusters in *n*-heptane was used here. In particular, each water cluster contained 100 water

molecules, and the continuum phase contained 388 *n*-heptane molecules. The diameter of the water clusters was about 1.4 nm, and the distance between them was about 0.6 nm. The naphthenic acid molecules were inserted into the water/*n*-heptane interfaces manually. The naphthenic acids (NPAs) employed here are defined as carboxylic monoacids, where the carboxylic acid group is attached to a cycloaliphatic structure through a short side chain[30] with a different number of carbons, say, from two to six. The chemical structure is shown as follows, where $n = 2, 3, 4, 5,$ and 6. The NPA we used for this part of the work is 6-methyl-2-naphthanepropionic acid (i.e., $n = 2$).

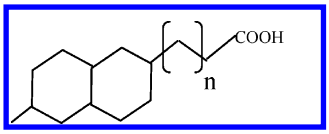

To reduce the computational requirements, the hydrophilic part of NPA was modeled as two charge carrying groups, the C═O and OH moieties. Here, the OH moiety is bonded to the carbonyl carbon. It should be emphasized again that the united carbon atoms on the hydrophobic part were also slightly charged since the charge equilibration method can only be performed on the whole molecule. Note that NPA is a weak acid and the dissociation of the COOH group into COO^- and H^+ ions was ignored here. In this way, the central processing unit times were significantly reduced as calculations of long-ranged ionic interactions were not required. It also mimicked, although not exactly, the experimental situation that water clusters are most stabilized in a high pH environment (i.e., minimal proton dissociation). In addition to the coulombic interactions, NPA and water molecules interact with each other through hydrogen bonding as well. When we inserted the NPA molecules into the interfaces, the hydrophilic part was oriented toward the water phase while the hydrophobic part to the *n*-heptane phase in order to reduce the relaxation time of the system to achieve thermodynamic equilibrium.

Two models with different numbers of adsorbed NPA molecules were built. In the first model, we used only 24 NPA molecules and they were all placed around one water cluster with the above-mentioned orientations while the interface of the remaining water cluster was free of NPA molecules. In the second model, we used 48 NPA molecules so that each water cluster was covered by 24 NPA molecules. It should be noted that since we inserted the molecules into the models manually, the spatial distribution of the NPA molecules over the corresponding interfaces was not totally uniform despite the fact that much effort had been attempted. The use of 24 NPA molecules was based on the work of Havre and Sjöblom on a similar surfactant using the Gibbs adsorption equation.[17] In particular, the authors determined that one NPA molecule could cover a surface area of about 52 $Å^2$ at room temperature. Given the size of the water clusters we used (diameter $\sim$ 1.4 nm), 24 NPA molecules would "fully" cover one water cluster. In addition to the above-described models, two similar models were also constructed using the densities of water and *n*-heptane at 80 °C (i.e., 0.97 and 0.64 g/cm^3) rather than those at 27 °C to determine the size of the periodic simulation box.[27] Therefore, the dimensions of the simulation boxes used at 80 °C were slightly larger than those at room temperature.

Note that the interfaces in the previous models possess a relatively high curvature compared to those of micrometer-sized water droplets in a similar experimental water-in-oil emulsion system. It may lead to an increased interfacial tension and bending resistance which could have an impact on the mobility of the molecules at the interface. To gain a more complete picture, a separate series of MD simulations was carried out by using flat water/*n*-heptane interfaces with naphthenic acids inserted in between. Here, we used NPAs with $n = 2-6$. The interface was created by assembling 100 water and 30 (or 70) *n*-heptane molecules together in an elongated periodic boundary box, as shown in Figure 1. The elongation process was performed to reduce artifacts originating from the interactions between the molecules in the parent simulation box and those in the image boxes in the vertical direction. Also, the naphthenic acids were inserted at the interface artificially with the hydrophilic head buried in the water molecules and the hydrophobic side buried in the *n*-heptane phase, respectively. The interface, with a fixed area of 18.5 × 18.5 $Å^2$, can only accommodate a maximum of about eight NPA molecules which is consistent with the finding of Havre and Sjöblom (a single NPA molecule could cover about 50 $Å^2$ at room temperature). The density of the simulation box before elongation was controlled by adjusting the length of the side perpendicular to the fixed interfacial area. In general, the initial configurations created in the foregoing described models, especially after the surfactant insertion process, are in a high energy state due to the overlapping of the van der Waals radii of the atoms. Energy minimizations, therefore, were required to relax all the structures before subsequent MD simulations by using a conjugate gradient method. Such energy minimization processes, albeit not necessarily a global minimum, would lead to a more uniform distribution of naphthenic acid molecules at the interfaces.

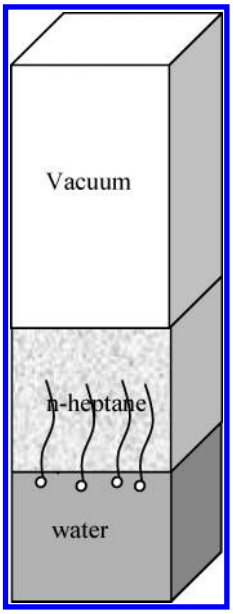

Figure 1. Schematics of the 3D periodic unit cell used in the modeling of the water/*n*-heptane interface with different numbers of surfactant molecules.

All MD simulations were performed in canonical (i.e., NVT) ensembles with initial velocities assigned randomly from a Maxwell−Boltzmann distribution at the temperature of interest. The modeled coalescence process was coupled to a simulated Nose thermal bath[27] with a time step of 1 fs to ensure the stability of the MD trajectory. Depending on the configuration of the model, various simulation times in the nominal value of 1000 ps per trajectory were used to relax the systems to their corresponding equilibrium state. The mean behavior of the naphthenic acids was obtained from an ensemble of 5 or 10 MD runs depending on the size of the models mentioned before. Independent trajectories were generated by choosing various sets of initial random velocities.

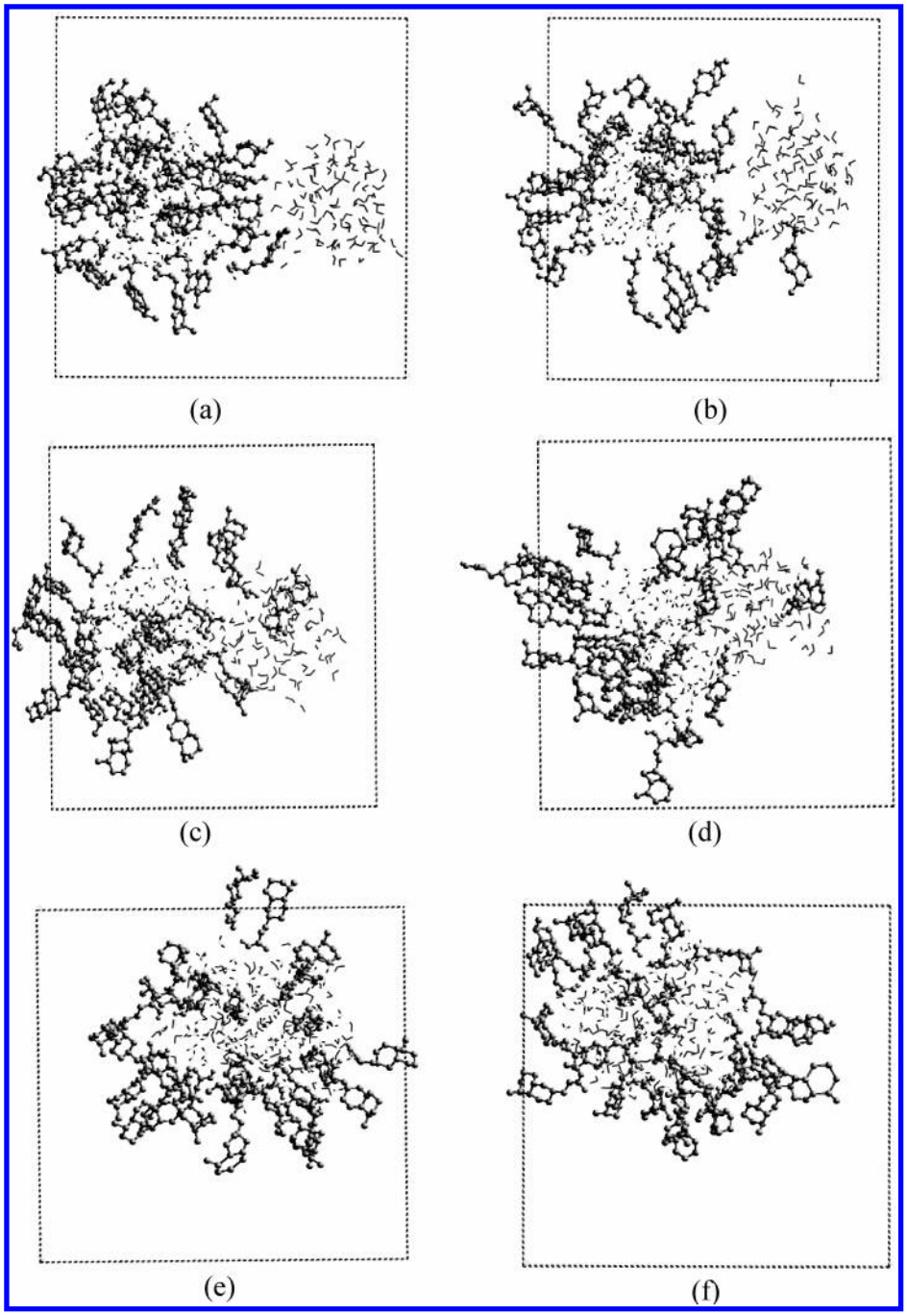

Figure 2. MD snapshots of the coalescence of two water clusters in *n*-heptane with one covered by 24 NPA molecules at 27 °C: (a) 1 ps, (b) 60 ps, (c) 70 ps, (d) 100 ps, (e) 300 ps, and (f) 700 ps.

3. Results and Discussion

3.1. Coalescence Mechanism. As mentioned, experimental results demonstrate that the high stability of residue water encountered in the oil production processes is attributed to the formation of a lamellar liquid crystalline phase (LLC) upon the adsorption of naphthenic acids and their salts. Also, it is believed that such a LLC phase reduces the mobility and bending ability of the interface. However, under nonequilibrium conditions, water droplets may not be covered completely by this LLC phase.[30] Water droplets thus could have an opportunity to coalesce. On the basis of this assumption, a corresponding model was built, with only 24 NPA molecules around one water cluster while the interface of the other was free of NPA molecules. Since our goal was merely to qualitatively image the coalescence mechanism at the molecular level, one MD run with the occurrence of coalescence was sufficient.

Figure 2 shows the snapshots of such a trajectory at 27 °C. The water molecules in the two clusters are displayed in different levels of gray with the shape of dots and rods, respectively, and the rendering of the NPA molecules is in the ball-and-stick form. *n*-Heptane molecules (i.e., the continuum phase) are not shown for easy viewing. In this figure, the two water clusters started to coalesce at around 70 ps. Compared to the induction time found in our previous work, a similar system with no adsorbed NPA (10 ps), the presence of NPA slowed the process considerably. Nonetheless, the total coalescence times for both systems are about the same, 300 ps. The process started when a couple of the NPA molecules moved slightly away from their original water/*n*-heptane interface, as shown in Figure 2b. Such

a movement, as a result of local density fluctuations, created an empty region between the two water clusters. Consequently, water molecules residing in the respective clusters moved into the empty region to form a mutual bridge through the long-ranged coulombic interaction, as shown in Figure 2c. The bonded and nonbonded energies did not exhibit any significant changes during this process, indicating that the diffusional motions are simply caused by the thermal energy available, not by the lowering of the total energy of the whole system. Since the two water clusters were deliberately placed near each other, the coalescence process did not require significant movements of the surrounding *n*-heptane molecules. With more *n*-heptane molecules between the water clusters, it is expected that the process would be further slowed and/or completely hindered since additional cooperative motions between the *n*-heptane and NPA molecules would be required to initiate the water bridge. However, as shown later in the Flat Interface Simulations section, when more *n*-heptane molecules are present in the vicinity of the water/*n*-heptane interface, the mobility of NPA molecules tends to be enhanced.

Once the bridge was formed, the two water clusters were triggered to approach each other to complete the subsequent coalescence process within a short period of time (300 ps). Upon completion of this process, all 24 NPA molecules stayed at the new interface formed between the resultant cluster and *n*-heptane until the end of the simulation (800 ps). With the simulation temperature increased to 80 °C, the rate of the coalescence process of the above system was increased as well. In particular, the process started at about 40 ps and completed at 150 ps rather than at 70 and 300 ps, respectively, as observed at 27 °C. The coalescence mechanism was essentially identical to what was observed at 27 °C. The additional thermal energy provided to the system shortened the induction time for the creation of the empty region as well as the coalescence time. The decrease in the coalescence time is simply attributed to the increase in the mobility of the NPA and water molecules.

3.2. Coalescence of Two Water Clusters Covered with NPA Molecules. Besides the previous model, the model with each water cluster covered by 24 NPA molecules was employed to simulate a more general case encountered in practice. Five trajectories were generated at 27 and 80 °C, respectively. Among the 10 MD trajectories, only 1 trajectory with the event of a full coalescence was found at 27 °C, as shown in Figure 3. In this figure, all carbon atoms including those of the NPA molecules have been deleted for clarity, NPA molecules thus are displayed in the ball form in the color of dark gray, and the water molecules in the two clusters are displayed in dots and rods, respectively, identical to what was shown in Figure 2. It can be seen that the coalescence process was substantially slowed even though the two clusters were nearby each other. Up to 300 ps, there was still no sign of the initiation of coalescence. It was up to 500 ps that a few NPA molecules from both clusters left their respective interfaces and were attracted to the *n*-heptane phase. Their hydrophilic heads formed a bridge and further attracted water molecules to strengthen the bridge. The coalescence process finished at 1100 ps which is much longer than the previous model. This indicated that even the mutual bridge between the water molecules had begun to be built up; the coalescence process was still slowed considerably. In this model, the number of NPA molecules is twice as many as that in the first model. This in turn limits the mobility of NPA and water molecules as the NPA molecules need to overcome the hydrogen bonds between their hydrophilic parts and the water molecules need to leave the interfaces (unlike the first model, no "new" hydrogen bonds could be formed in this model). The results suggest that the occurrence of the coalescence is a low-probability event, even at 80 °C, which appears to be consistent with the experimental observations.[4,5]

From all the above simulations, we can see that the departure of NPA molecules from the water/*n*-heptane interface is an essential step for the coalescence process. Therefore, to some extent, the coalescence process could be quantitatively distinguished by the mobility of the NPA molecules. Here, we used the diffusion coefficients (D) to achieve our purpose. They were calculated based upon their average mean-squared displacements over the time period in which coalescence took place. The detailed calculation procedure has been described elsewhere.[1] Moreover, to ensure whether our simulation time was long enough for NPA molecules to move in a real random walk fashion, we calculated their velocity autocorrelation functions for the second water cluster model as well as a flat interface model, both at 80 °C. As shown in Figure 4, the correlation time for the water cluster model was only 1.1 ps, demonstrating that a nominal simulation time of 1000 ps was long enough to guarantee a random walk of the acid. It should be noted that the velocity autocorrelation time for the flat interface model, which was not reported here, is comparable to that of the second water cluster model. Nonetheless, we would like to alert the reader that the diffusion coefficients we calculated here using the Einstein equation are merely used to quantify the mobility of the molecules involved during the coalescence process (a nonequilibrium process) and they should not be considered as equilibrium diffusion coefficients of the individual components involved since coefficients obtained in this work are system specific, depending on the configuration and concentrations of various components in the system.

Table 2 summarizes the calculated diffusion coefficients of NPA for the aforementioned models along with the corresponding results for water and *n*-heptane at the chosen simulation temperatures. For the MD runs used for the second model where no coalescence occurred, the diffusion coefficients were calculated as the average over the corresponding ensembles, while the diffusion coefficients for the first model and the second model with the occurrence of coalescence were calculated based upon only one MD trajectory. According to the data shown in Table 2, a more detailed picture of the coalescence mechanism emerges as follows:

(a) Dynamics of NPA molecules. For the MD trajectories with the occurrence of coalescence in both models, the mobility of NPA is much lower than that of water and *n*-heptane. This is simply due to the fact that the motions of NPA molecules were more or less restricted within the interfacial region while the other components were not, especially *n*-heptane. On the contrary, for the trajectories without coalescence (i.e., the second model), the mobility of NPA is higher than that of water. This considerably reduces the chance for the formation of a water bridge. However, regardless of the temperature, diffusion coefficients of NPA for the first model are much higher than those of the second one, indicating that NPA at low interfacial concentrations has a higher mobility that would facilitate the formation of a water bridge so long as its mobility is lower than that of the water.

(b) Dynamics of *n*-heptane molecules. The diffusion coefficient of *n*-heptane in the first model at 27 °C was 0.42 $Å^2$/ps, which is quite close to its experimental self-diffusion coefficient value of 0.44 $Å^2$/ps, indicating that the presence of the NPA and water molecules did not affect their mobility during the coalescence process. Yet when we increased the amount of NPA

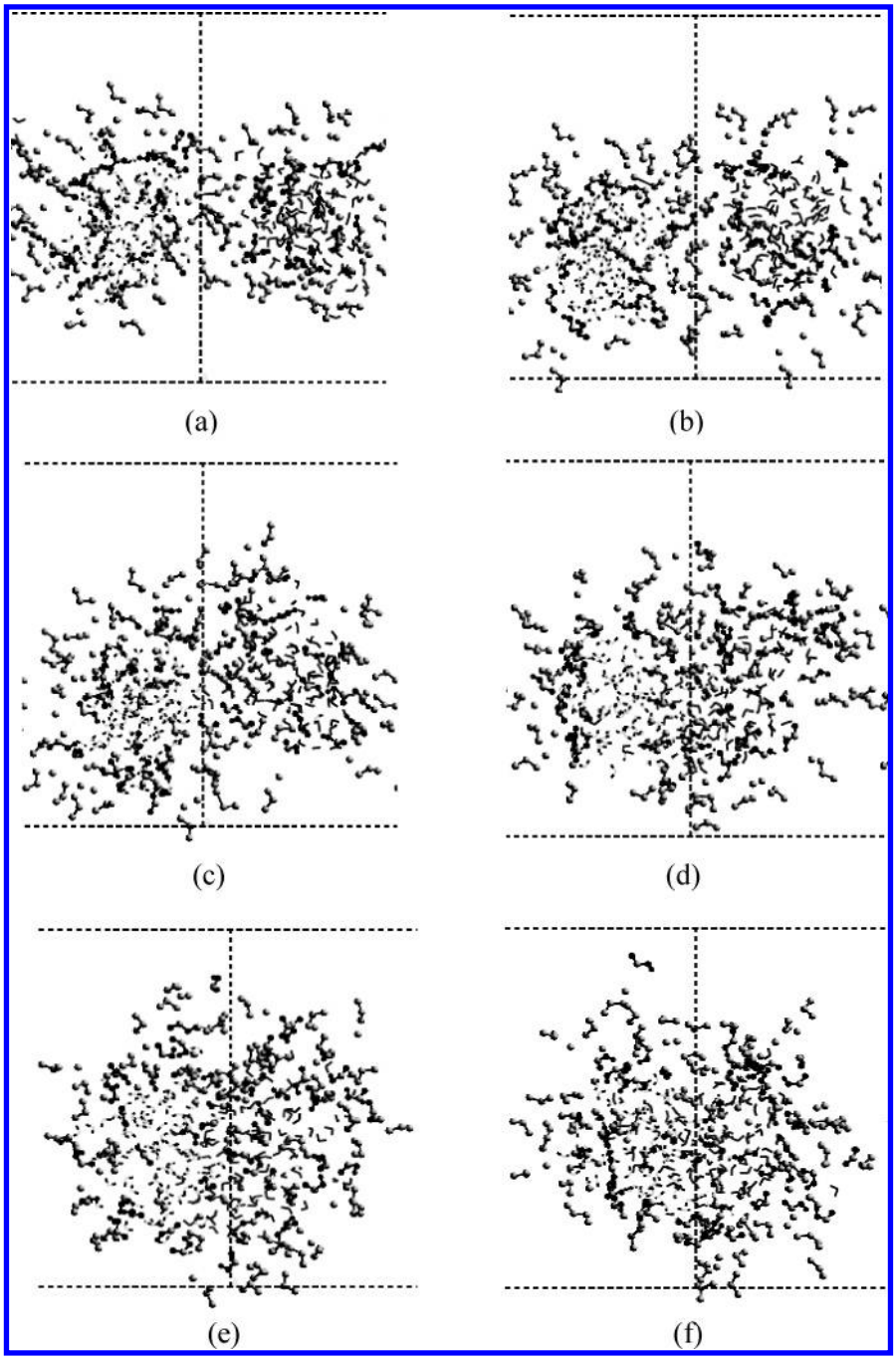

Figure 3. MD snapshots of the coalescence of two water clusters in *n*-heptane with each covered by 24 NPA molecules: (a) 1 ps, (b) 300 ps, (c) 500 ps, (d) 700 ps, (e) 900 ps, and (f) 1100 ps.

in the second model, the diffusion coefficients of *n*-heptane were significantly reduced, especially in the noncoalescence trajectories. This is reasonable as the water bridge would be difficult to form without the cooperative motions of the *n*-heptane molecules.

(c) Dynamics of water molecules. In Table 2, water molecules are classified into three categories: water in NPA, water without NPA, and bridging water. Their corresponding diffusion coefficients were calculated separately. In the first model, the *D* value of the water molecules without NPA (0.24 $Å^2$/ps) is very close to its experimental self-diffusion coefficient (0.26 $Å^2$/ps). Compared to this value, the water molecules inside the cluster with adsorbed NPA molecules moved at a much lower diffusion rate (0.15 $Å^2$/ps). Likewise, for the trajectory with coalescence in the second model, a similar diffusion coefficient of water in NPA is observed (0.14 $Å^2$/ps). This may be attributed to the additional hydrogen bonds formed with the surrounding NPA molecules. In the three trajectories in which coalescence occurred, the mobility of the bridging water molecules was even lower than that of the water in NPA. This low mobility suggests that the water bridge formed between two water clusters could be easily broken by the NPA molecules during the coalescence process. In fact, such a water bridge breaking process was observed in the simulations of the second model, wherein the NPA molecules between two water clusters left the water/*n*-heptane interfaces frequently, yet covered them back again immediately, thus interrupting the coalescence process. This leads to a much slower coalescence process or the diminishment of the coalescence probability.

In summary, the results from these simulations suggest that NPA slowed the initiation process not only by acting as a steric barrier for the water bridge formation but also by decreasing

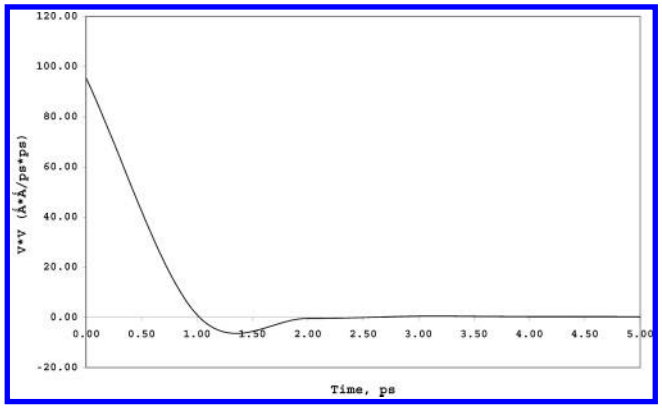

Figure 4. Velocity autocorrelation function of the second water cluster model with 48 NPA ($n = 2$) molecules at the curved water/*n*-heptane interfaces at 80 °C.

the mobility of the bridge water molecules and the water in NPA. In fact, with the introduction of more NPA molecules into the system (e.g., model 2), the diffusion coefficient of *n*-heptane was also reduced. This implies that *n*-heptane may play a more important role in determining the kinetics of the coalescence process in the second model than that for the first one. In addition, the mobility of all the components involved in these two models exhibited positive temperature dependence, especially for the model of two water clusters both covered with adsorbed NPA molecules. It is consistent with the experimental observation that the application of elevated temperatures is an effective means to destabilize certain interfaces.

3.3. Flat Interface Simulations. The curvature of the water clusters described previously is substantially higher than that of the model experimental systems. This high curvature plus high interfacial tension between water and *n*-heptane may affect the mobility of the NPA molecules. Moreover, a visual inspection of the orientations of the NPA molecules in the above models does not indicate any liquid-crystal-like packing at the interface. To address these two issues, we carried out a separate series of MD simulations using infinite flat water/*n*-heptane interfaces at 80 °C with adsorbed naphthenic acids. The naphthenic acids adopted here contained a cycloaliphatic structure which is connected to a carboxylic acid with a short side chain of two to six carbons (*n* from 2 to 6). The interface was created by assembling 100 water and 30 *n*-heptane molecules together in an elongated periodic boundary simulation box. The decision to use 30 *n*-heptane molecules was made based on the number of *n*-heptane molecules present between the water clusters in the previous models. The number of water molecules was chosen based on the criterion that the bulk density of water could be recovered in the interior of the water layer in the elongation direction. For each naphthenic acid, the average diffusion coefficient was calculated from an ensemble of 10 trajectories, as shown in Figure 5.

As shown in this figure, the diffusion coefficient of the naphthenic acid with $n = 2$ is about 0.0090 Å^2/ps which is fairly comparable to that for the same NPA adsorbed at the highly curved interface (0.0099 Å^2/ps at 80 °C). The finding suggests that the mobility of NPA at the interfacial region was not sensitive to the curvature of the interface, at least at high NPA concentrations. The result is somewhat unexpected. Further investigations are required to discern the cause for such an observation. It can also be noted from this figure that, with increasing *n*, the mobility of naphthenic acid is slightly reduced, yet this decrease is moderate (from 0.008978 to 0.006083 Å^2/ps). As mentioned, a similar observation was obtained in experiments in which emulsion stability was found to be weakly dependent on the molecular weight of naphthenic acids[11−17] and the naphthenic acids with high molecular weight seem to have slightly better stabilizing abilities.[17]

To quantify the order present at the water/*n*-heptane interface, we calculated the corresponding order parameter (*S*) of the naphthenic acids. Conventionally, the order parameter is given as follows

$$S = \frac{1}{2}\langle 3\cos^2\theta - 1\rangle \qquad (2)$$

where θ is the angle between the director and the long axis (e.g., *z* axis) of the molecules of interest. The brackets denote an average over all of the molecules in the sample. The θ calculated here is the angle between the direction of every C−C bond in the side chain and the *z* axis, along which naphthenic acids were artificially inserted into the interface. As for the cycloaliphatic part, it was considered as a unit with θ defined as the angle between the *z* axis and the axis on the cycloaliphatic plane along the direction of the side chain. In the case when the noncoplanar circumstance of the cycloaliphatic plane happened during the simulation, the whole axis was divided into two parts by the center of the entire plane, the *S* value of each part was calculated independently. Thus, the order parameter of each molecule was calculated by averaging the order parameters obtained from various parts of the molecule using the above equation. In an isotropic liquid, the order parameter is close to zero whereas it evaluates to 1 for a perfect crystal. Typical values for the order parameter of a liquid crystal range from 0.3 to 0.9. Table 3 summarizes the order parameters of the naphthenic acids with *n* from 2 to 6 for a MD trajectory randomly selected from the 10 trajectory ensemble. Each value was obtained by averaging over 10 frames every 10 ps in the last 100 ps (i.e., from 900 ps to 1000 ps) with the corresponding standard errors. In this table, the order parameters of all naphthenic acids are around 0.5, indicating that a LLC phase existed at the water/*n*-heptane interfaces which confirms previously mentioned experimental observations.[6−17]

In addition to the simulations above, we created a flat water/*n*-heptane interface by augmenting the number of *n*-heptane molecules from 30 to 70 to discern the effect of the amount of *n*-heptane molecules near the water/*n*-heptane interface on the mobility of NPA. For this new interface, simulations using NPA molecules with $n = 2$ (the NPA molecule used in the first water cluster model) were performed. This simulation could be pictured as two water droplets far apart from each other. The resultant mean diffusion coefficient of NPA was 0.041 ± 0.005 Å^2/ps, also calculated from an ensemble of 10 MD trajectories. This value is almost 1 order of magnitude higher than that of the interface with 30 *n*-heptane molecules (0.009 ± 0.001 Å^2/ps). The result led us to propose that the departure of naphthenic acids is hindered by the *n*-heptane molecules when water clusters are in close proximity, whereas the process is facilitated by the departure of the acids (higher mobility) when water clusters are far apart from each other.

4. Concluding Remarks

Molecular dynamics simulation was used to study the stability of nanometer-sized water clusters in *n*-heptane, with the full coverage of adsorbed 6-methyl-2-naphthatenepropionic acid at the water/*n*-heptane interfaces, at two temperatures. It was found that coalescence of the water clusters was entirely due to the diffusional motion of the components involved which required the initial departure of the acid molecules from the interface leading to the formation of a water bridge. Our simulations show

TABLE 2: Calculated Diffusion Coefficients (*D*) of Water, NPA, and *n*-Heptane for the Two Models at 27 and 80 °C as Described in the Text

		diffusion coefficient $\langle D \rangle$ (Å^2/ps)[a]				
	temperature (°C)	water in NPA	water without NPA	bridging water	NPA	*n*-heptane
one cluster with adsorbed NPA	27	0.15	0.24	0.10	0.11	0.42
	80	0.29	0.34	0.13	0.12	0.55
two clusters with adsorbed NPA (with coalescence)	27	0.14	N/A	0.087	0.043	0.27
two clusters with adsorbed NPA (without coalescence)	27	0.0021 ± 0.0003	N/A	N/A	0.0058 ± 0.0003	0.110 ± 0.003
	80	0.0037 ± 0.0003	N/A	N/A	0.0099 ± 0.001	0.230 ± 0.010

[a] The *D* values for the first model were calculated from one trajectory; while for the MD runs without coalescence in the second model, the average *D* values were obtained from the ensembles of four (27 °C) and five (80 °C) trajectories with the corresponding standard errors. The *D* values for the second model with coalescence are also shown here.

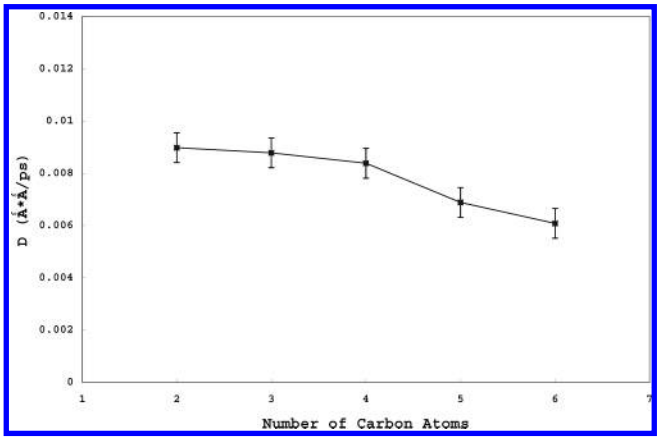

Figure 5. Average diffusion coefficients calculated from an ensemble of 10 MD trajectories for naphthenic acids with the alkyl side chain with 2−6 carbons connecting the cycloaliphatic structure and the carboxylic acid group.

TABLE 3: Computed Order Parameters of Naphthenic Acids ($\langle S \rangle$) with Various Alkyl Side Chains ($n = 2-6$ carbons) Connecting the Cycloaliphatic Structure and Carboxylic Acid Group[a]

n	$\langle S \rangle$	STDE
2	0.477	0.021
3	0.506	0.010
4	0.560	0.011
5	0.521	0.006
6	0.510	0.005

[a] Each value was obtained by averaging over 10 snapshots taken from every 10 ps of the last 100 ps of the corresponding trajectories with the associated standard errors (STDE).

that the coalescence of two water clusters fully covered by 6-methyl-2-naphthatenepropionic acid molecules was a low-probability event even at evaluated temperatures, which is consistent with experiment. NPA molecules present at the water/*n*-heptane interface not only acted as a steric barrier for the coalescence process but also slowed the motions of the water and *n*-heptane molecules in their immediate vicinity. Although the diffusion coefficients of all the components involved increased with increasing temperature, suggesting that the use of elevated temperatures should be an effective means to destabilize water/*n*-heptane interfaces, the mobility of water in such a situation is much lower than that of naphthenic acids, making the formation of a water bridge rather difficult.

Results obtained from the flat interface models indicate that the emulsion stability was weakly dependent on the molecular weight of the naphthenic acid utilized. The calculated order parameters of the naphthenic acids used in this work reinforce the experimental observation that they form liquid-crystal-like ordering at the water/*n*-heptane interface. Interestingly, our work offers an additional insight about the role of naphthenic acids in the stabilization mechanism; that is, the mobility of the naphthenic acids is considerably lowered (more stable) when the water clusters are in close proximity whereas their mobility is enhanced by 1 order of magnitude when water clusters are surrounded by more *n*-heptane molecules. In the latter case, coalescence could not occur as the water clusters are far apart from each other.

Acknowledgment. The financial support through a COURSE grant from the Alberta Energy Research Institute is gratefully acknowledged. This research has been enabled by the use of WestGrid computing resources, which are funded in part by the Canada Foundation for Innovation, Alberta Innovation and Science, BC Advanced Education, and the participating research institutions. WestGrid equipment is provided by IBM, Hewlett-Packard, and SGI.

References and Notes

(1) Zhao, L.; Choi, P. *J. Chem. Phys.* **2004**, *120*, 1935.
(2) Goldszal, A.; Hurtevent, C.; Rousseau, G. *SPE Oilfield Scale Symposium*; SPE74661, Aberdeen, U.K., 2002.
(3) Rousseau, G.; Zhou, H.; Hurtevent, C. *SPE Oilfield Scale Symposium*; SPE68307, Aberdeen, U.K., 2002.
(4) Hsu, C. S.; Dechert, G. J.; Robbins, W. K.; Fukuda, E. K. *Energy Fuels* **2000**, *14*, 217.
(5) Acevedo, S.; Escobar, G.; Ranaudo, M. A.; Khazen, J.; Borges, B.; Pereira, J. C.; Mendez, B. *Energy Fuels* **1999**, *13*, 333.
(6) Friberg, S.; Mandell, L.; Larsson, M. *J. Colloid Interface Sci.* **1969**, *29*, 155.
(7) Friberg, S. *J. Colloid Interface Sci.* **1971**, *37*, 291.
(8) Friberg, S.; Mandell, L. *J. Pharm. Sci.* **1970**, *59*, 1001.
(9) Friberg, S.; Jansson, P. O.; Cederberg, E. *J. Colloid Interface Sci.* **1976**, *55*, 614.
(10) Friberg, S.; Solans, C. *Langmuir* **1986**, *2*, 121.
(11) Urdao, O.; Sjöblom, J. *J. Dispersion Sci. Technol.* **1995**, *16*, 557.
(12) Schildberg, W.; Sjöblom, J.; Christy, A. A. *J. Dispersion Sci. Technol.* **1995**, *16*, 575.
(13) Saeter, O.; Sjöblom, J. *Colloid Polym. Sci.* **1999**, *277*, 541.
(14) Mouraille, O.; Skodvin, T.; Sjöblom, J.; Peytavy, J. L. *J. Dispersion Sci. Technol.* **1998**, *19*, 339.
(15) Friiso, T.; Schildberg, Y.; Rambeau, O.; Tjomsland, T.; Forderal, H.; Sjöblom, J. *J. Dispersion Sci. Technol.* **1998**, *19*, 93.
(16) Gundersen, S. A.; Sjöblom, J. *Colloid Polym. Sci.* **1999**, *277*, 462.
(17) Havre, T. E.; Sjöblom, J. *Colloids Surf., A* **2003**, *228*, 131.
(18) Horvath-Szabo, G.; Czarnecki, J.; Masliyah, J. H. *J. Colloid Interface Sci.* **2001**, *236*, 233.
(19) Horvath-Szabo, G.; Masliyah, J. H.; Czarnecki, J. *J. Colloid Interface Sci.* **2001**, *242*, 247.
(20) Horvath-Szabo, G.; Czarnecki, J.; Masliyah, J. H. *J. Colloid Interface Sci.* **2002**, *253*, 427.
(21) Dominguez, H. *J. Phys. Chem. B* **2002**, *106*, 5915.

(22) Urbina-Villalba, G.; Garcia-Sucre, M. *Langmuir* **2000**, *16*, 7975.
(23) Accerlys Inc., San Diego, CA.
(24) Mayo, S. L.; Olafson, B. D.; Goddard, W. A., III. *J. Phys. Chem.* **1990**, *94*, 8897.
(25) Rappe, A. K.; Goddard, W. A., III. *J. Phys. Chem.* **1991**, *95*, 3358.
(26) Ryckaert, J. P.; Bellemans, A. *Chem. Phys. Lett.* **1975**, *30*, 123.
(27) Yaws, C. L. *Thermodynamic and Physical Property Data*; Gulf Publishing Co.: Houston, TX, 1992.
(28) Nose, S. *J. Chem. Phys.* **1984**, *81*, 511.
(29) Bobbins, W. K. *Abstr. Pap. Am. Chem. Soc.* **1998**, *215*, 019-PETR.
(30) Horvath-Szabo, G.; Czarnecki, J.; Masliyah, J. H. *J. Colloid Interface Sci.* **2002**, *253*, 427.